

# Determination of the Modern Marine Gas Turbine Rotor Forced Vibration Parameters by Numerical and Experimental Methods

Nour Hider Almarahleh<sup>1</sup>, Mahmoud M. S. Al-suod<sup>2,3,\*</sup>, Serhii Morhun<sup>4</sup>, Natalia Smetankina<sup>5</sup>, Iryna Zhuk<sup>6</sup>, Yurii Zolotyi<sup>4</sup>, and Razan Haedar Al Marahla<sup>7</sup>

<sup>1</sup> Department of Civil Engineering, Tafila Technical University, Tafila, Jordan

<sup>2</sup> Electrical Engineering Department, Al-Ahliyya Amman University, Amman, Jordan

<sup>3</sup> Department of Electrical Power Engineering and Mechatronics, Tafila Technical University, Tafila, Jordan

<sup>4</sup> Department of Applied Mechanics, Admiral Makarov National University of Shipbuilding, Mykolaiv, Ukraine

<sup>5</sup> Department of Vibration and Thermostability Studies, Institute of Power Machines and Systems, Kharkiv, Ukraine

<sup>6</sup> Department of Higylene, Social Medicine, Public Health and Medical Informatics,

Petro Mohyla Black Sea National University, Mykolaiv, Ukraine

<sup>7</sup> Department of Civil and Infrastructure Engineering, Al-Zaytoonah University of Jordan, Amman, Jordan

Email: nour@ttu.edu.jo (N.H.A.), m.alsuod@ammanu.edu.jo (M.M.S.A.-S.), m.alsoud@ttu.edu.jo (M.M.S.A.-S.),

serhii.morhun@nuos.edu.ua (S.M.), nsmet@ipmach.kharkov.ua (N.S.), iryna.zhuk@chmnu.edu.ua (I.Z.),

goldspekl@ukr.net (Y.Z.), r.almarahla@zuj.edu.jo (R.H.A.M.)

Manuscript received July 18, 2025; revised September 23, 2025; accepted November 26, 2025

\*Corresponding author

**Abstract**—The paper is devoted to the turbomachinery vibration processes investigation. It is based on the hypothesis that such process as forced vibration, high temperature and centrifugal force, constructional damping parameters put the main impact in the gas turbine rotors decrease. For these studies the special refined mathematical model was used. For these model the special space finite elements have been developed, that gives an opportunity to make the approximation of various turbine blades geometry. The model verification has been done by the usage the modern highly automatized experimental equipment that is based on the holographic interferometry method application in real time. The first impeller cooled blades forced vibration parameters have been determined for several most dangerous forced vibration modes, temperatures up to 1000°C and angular velocities of shaft rotation, corresponding with the gas turbine engine normal working regime. Results of calculations data together with the previous studies in the fields of gas turbine engines flow dynamics, heat exchange, stress-strain state can be used in further studies of turbomachinery fracture mechanics area.

**Index Terms**—turbomachinery rotors, forced vibration, gas flow temperature, centrifugal force, constructional damping, durability

## I. INTRODUCTION

Marine gas turbine engine rotors operate in very adverse conditions that arise as a result of the simultaneous action of a number of negative factors and cause the appearance of forced vibration and dynamic stresses in the rotor elements. Such factors include the influence of high-speed turbulent gas-dynamic flow, high temperatures on the surfaces of the impellers due to heat exchange between the flow and the rotor, temperature gradients due to cooling of

the first impeller blades, the centrifugal force impact to the rotor forced vibration.

It should be noted that the systems of equations describing the forced vibration processes and the stress-strain state of the rotor do not have an analytical solution, therefore, numerical methods should be used. Also, the use of numerical modeling to determine the modes and frequencies of forced vibration and the stress-strain state in the GTE rotors allows to determine stress concentrators and develop recommendations for their elimination at the stages of design documentation developing. Thus, in paper the harmonic response analysis on the base of Finite Elements Method (FEM) has been done, but the processes of heat exchange between blades and flow, that cause thermal stresses in rotor has not been studied [1]. Chen *et al.* [2] the authors used numerical methods for marine gas turbine engine shock resistance analysis in a wide range of sea waves amplitudes. Also numerical methods, especially FEM are used by many scholars for blades modal analysis not only in marine technique but in other areas of engineering too [3].

Numerical analysis based on mathematical models that take into account all negative factors, that cause the gas turbine rotor forced vibration, allows to reduce the number of necessary multi-valued full-scale experiments and increase the whole GTE durability.

## II. METHODOLOGY

### A. Experimental Methods

Experimental studies of turbomachine blades resonant vibrations were performed to assess the adequacy of the developed mathematical models and calculation methods, to check the reliability of the accepted hypotheses and the

accuracy of the obtained numerical results, and to identify features of the influence of design inhomogeneities on the main dynamic characteristics of the models under consideration that cannot be theoretically analyzed. Cooled and uncooled working blades of turbomachines with different geometric parameters and design features were studied. To conduct this study, the holographic interferometry method was used according to the technique described in [4], which allows to record the areas of displacement distribution with the order of the wavelength amplitude of the light source. The use of this method in studying deformations and vibration displacements is suitable due to its exceptionally high accuracy and reliability compared to traditional labor-intensive and insufficiently reliable, especially in the area of high vibration frequencies, contact methods, such as scanning with a vibration probe, strain gaging, and the use of optically sensitive and fragile coatings. The disadvantages of this method include the complexity of the hardware complex servicing the holographic stand and the impossibility of directly measuring the vibration amplitudes using a holographic interferogram.

Time averaging method. In this case, the oscillating object is recorded on a hologram when illuminated by a continuous light stream. In the extreme positions, the points of the blade surface are in a longer period of time than in all intermediate positions, therefore, on the hologram they are usually recorded in amplitude positions. The movement of the points in the intervals between these positions leads to a Doppler shift in the frequency of the light wave, and the incoherent illumination that occurs in this case sharply reduces the contrast of the interference bands. And only those points that are in the vibration nodes have high brightness in the reflected image [5].

Real time method. When observing the interferogram of a vibrating object in real time, a variable pattern of bands is obtained, averaged by a photo recorder. That is, instead of averaging the complex amplitude of the light wave, carried out in the time averaging method, the resulting intensity of the light wave is averaged. Comparison of these two methods shows that the brightness and contrast of the fringes when observing oscillations in real time is significantly lower, and the distance between the fringes is twice as large as on the time-averaged interferogram, i.e. the main disadvantages of the time-averaging methods and the real-time observation method are the sharp decrease in the brightness and contrast of the interference fringes with an increase in the oscillation amplitude. In practice, it is possible to distinguish fringes no higher than the 10th – 15th order [6], which significantly complicates obtaining quantitative information on the distribution of oscillation amplitudes over the surface of the object under study.

Strobe-holographic method. Its essence lies in the fact that the strobated radiation is synchronized with the amplitude moments of vibration, i.e. on the hologram the vibrating blade will be fixed only in two amplitude positions. In comparison with the above methods, it increases the contrast of the interference fringes and the resolution of the photo image, which allows their subsequent decoding for the purpose of quantitative

interpretation of the obtained interference patterns, as well as increasing the maximum permissible amplitude of oscillations of the model. Strobing also ensures the same modulation of the intensities of the object and reference beams. The peculiarity of the method is that the object under study is illuminated by a laser beam at moments in time when the points of the surface of the oscillating zones are in one of the extreme amplitude positions and the strobe-hologram is exposed at specified moments in time. In this case, the light pulses are synchronized with the specified phase of oscillations. The strobing frequency is selected as a multiple of the oscillation frequency of the model under study. The duration of the strobe pulse is set equal to a part of the oscillation period and is synchronized with one of the extreme amplitude positions of the model, in which the strobe interferogram is exposed. Therefore, the contrast of the interference fringes does not depend on the oscillation amplitude. The disadvantage of this method is the difficulty in determining the interference maxima, since the brightness of all the bands is high.

The speckle interferometry method is a method of optical non-destructive testing based on the analysis of speckle structures formed by the reflection of coherent optical radiation from the surface of an object (blade). A specific speckle structure contains information about the micro relief and shape of the object. By statistically processing the spotted structure, it is possible to obtain information about the parameters of the object's movement, including its displacements, speed of movement, amplitude and frequency of its vibrations, etc. The advantage of surface research methods using speckle structure is the possibility of studying systems that are inaccessible for direct observation in order to measure the parameters of the micro relief, shape and displacements, with the comparative simplicity of the technical implementation of these methods [4, 6, 7].

Summarizing the given above information it should be made a conclusion, that for the marine gas turbine rotor elements forced vibration experimental study the speckle interferometry method is the most useful and adequate, in future work we can do analysis and control using Artificial-Intelligence-Based and fuzzy logic control [8, 9].

## B. Numerical Methods

Since the advent of the finite element method (FEM), one of the areas of its application has been strength calculations. Performed finite element modeling (FEM) using three-dimensional software like ANSYS/CFX and validated the results against laboratory to validate the numerical models and allow for controlled variation of parameters [10]. The properties of finite element models are determined by the finite elements used and, depending on the blades under study, existing or new finite elements were developed [11]. Thus, the author of [12] used quadrangular bending elements of plates to analyze the vibration behavior of blades presented in the form of twisted cantilever plates in the field of centrifugal forces. Such elements are suitable only for objects that are surfaces of revolution. In [13], rectangular finite elements of constant thickness were used to study the natural vibrations of an untwisted nozzle blade of a gas turbine.

The authors of [14] applied FEM to determine the characteristics of free vibrations of cantilever blades of a gas turbine, using cylindrical shell elements, each of which has 28 degrees of freedom. In [15], flat triangular elements with three nodes and six degrees of freedom at each node were used to calculate the frequencies and modes of oscillation of steam turbine blades in a centrifugal force field. The same element was used to analyze the natural oscillations of a centrifugal compressor impeller in [16]. The authors of [16] modeled a compressor blade using triangular elements. These elements have three nodes at the vertices of the triangle with six degrees of freedom at each of them. The authors of [17] developed and investigated curved beam elements with different twist angles and different cross sections, which have two nodes with four degrees of freedom at each node and are used to analyze the oscillations of short twisted blades of large thickness. In [18], conical beam elements were developed, for improving the properties of which, within the element, an approximation of the displacement field using fifth-degree polynomials is applicable.

The authors of [19] used triangular finite elements of variable thickness with a flat middle surface to study the oscillations of gas turbine engine blades in non-stationary flow. The finite elements, which are used to obtain the frequencies and shapes of free oscillations in the field of centrifugal forces, contain three nodes at the corners of the middle surface with seven degrees of freedom at each node (three displacements and three rotation angles). The application of FEM to some classes of problems is complicated by the presence of complex-configured boundaries of the studied regions. In these cases, it is necessary to reduce the size of the elements and increase their number, which complicates the problem. Therefore, the authors of [20] developed a triangular bending element of a plate, which differs from the previously considered triangular elements by the presence of one curvilinear boundary. The authors of [21] used FEM to study the vibration behavior of pre-twisted working blades with cracks, presented in the form of flat cantilever plates. They modeled a pre-twisted plate by a set of triangular elements of constant thickness with nine degrees of freedom.

The authors of [22] developed a curved shell-type finite element for calculating the free oscillations of turbomachine blades. The use of this type of element made it possible to model objects of complex geometry and take into account the effect of transverse deformation. A similar element was developed by the authors of [23] taking into account the effects of rotations, excluding the influence of Coriolis acceleration. For the elements described above, the FEM relationships could be obtained by analytical methods, since the integration was carried out over a volume with simple boundaries. In the case of more complex curvilinear elements, this problem can only be solved using quadrature formulas for numerical integration, the order of the schemes of which has a noticeable effect on the accuracy of the models. In [24], various numerical integration schemes were studied when calculating the mass matrices and stiffness of curvilinear shell elements. Good agreement between the calculation results and the

experiment was noted when using the Gauss quadrature formula. The number of integration points in Gauss integration scheme is equal to two for each coordinate axis.

### III. RESEARCH OBJECT AND AIMS

The research object is the marine gas turbine rotor forced vibration frequencies spectrum. The impact of factors, caused by the engine operation process on the rotor durability decrease is studied, taking into account constructional damping. Turbine rotor is considered as a part of a solid continuum. These continuum energy imbalance during the turbine operation process is studied on the base of computational fluid dynamics, heat exchange, mechanics of solids scientific areas and causes the rotor forced vibration. The influence of centrifugal force also causes the additional mechanical extension of the impellers.

Gas turbine rotor durability is sharply decreased by the influence of above mentioned negative factors and should be precisely studied. To achieve a significant progress in such studies we need to:

- On the base of numerical methods develop the gas turbine rotor blades vibration mathematical model;
- Experimentally verify the developed model
- Study the processes of convective heat exchange between the flow and rotor blades;
- Study the blades forced vibration, taking into account damping processes in the rotor;
- Determine the centrifugal force, causing rotor blades additional extension;
- Define the complex influence of all the above mentioned negative factors on the rotor durability.

### IV. MATHEMATICAL MODEL FORMATION

#### A. Formulation of the Problem

Gas turbine rotor as a solid body can be considered in the Newtonian frame Cartesian coordinate system (Fig. 1). Thus according to the d'Alembert's principle it has a constant angular velocity  $\omega$ . The blades are mounted on the disks of the same radius  $R$ .

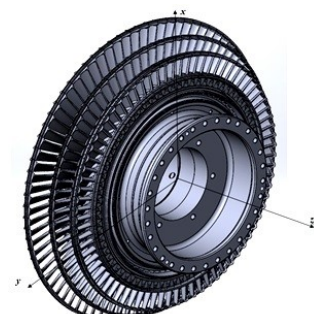


Fig. 1. The three-dimensional model of the turbine rotor.

The gas turbine rotor modal analysis is done, using the canonical equation of solid continuum vibration in matrix form:

$$\mathbf{M} \frac{d^2}{dt^2} \mathbf{\delta} + \mathbf{C} \frac{d}{dt} \mathbf{\delta} + \mathbf{K} \mathbf{\delta} = \mathbf{p} + \mathbf{F} \quad (1)$$

where  $\mathbf{M}$  is the mass matrix;  $\mathbf{C}$  is the damping matrix;  $\mathbf{K}$  is the stiffness matrix;  $\mathbf{p}$  is the vector of the flow pressure;  $\mathbf{F}$  is the vector of centrifugal forces;  $\boldsymbol{\delta}$  is the rotor generalized displacement vector.

The gas turbine rotor under study consists of three impellers, made without misalignments between the contacting blades, so it has cyclic symmetry.

### B. Determination of the Centrifugal Force Vector

The field of flow pressure determination using hexagonal finite elements and the turbine rotor approximation by these elements have been detailed described in the paper [24]. Such finite elements are also used for the centrifugal forces field determination.

Within the selected finite element, we select an elementary unit volume  $\rho dV$ . The vector of centrifugal forces  $d\mathbf{F}$  developed by the mass  $\rho dV$  is expressed as follows:

$$d\mathbf{F} = \begin{bmatrix} dF_x \\ dF_y \\ dF_z \end{bmatrix} \quad (2)$$

where  $dF_x$ ,  $dF_y$ ,  $dF_z$  are projections of the centrifugal force vector on the Cartesian coordinate axes.

Let us write down expressions for the components of the centrifugal force vector:

$$\begin{aligned} dF_x &= \rho dV \Omega^2 (R + x + \delta_x) \\ dF_y &= \rho dV \Omega^2 (y + \delta_y) \\ dF_z &= 0 \end{aligned} \quad (3)$$

where  $\rho$  is the blade material density;  $V$  is the blade volume;  $\delta_x$ ,  $\delta_y$  are projections of the generalized displacement vector on the Cartesian coordinate axis;  $x$  and  $y$  are coordinates of each finite element node in the rotor global coordinate system;  $R$  is the radius of impeller.

### C. Study of the Convective Heat Exchange between Rotor and Gas Flow

Using the Lagrange variation principle the rotor temperature field is determined [15, 21]:

$$\frac{\partial}{\partial x} \left( \lambda_x \frac{\partial T}{\partial x} \right) + \frac{\partial}{\partial y} \left( \lambda_y \frac{\partial T}{\partial y} \right) + \frac{\partial}{\partial z} \left( \lambda_z \frac{\partial T}{\partial z} \right) + Q = C_T \rho \frac{\partial T}{\partial t} \quad (4)$$

where  $T$  is the blade surface temperature;  $Q$  is the internal heat flux;  $C_T$  is the blade material specific heat;  $\lambda_x$ ,  $\lambda_y$ ,  $\lambda_z$  are thermal conductivity coefficients according to the  $x$ ,  $y$ ,  $z$  axis in  $\text{Wt}\cdot\text{m}/\text{K}$ ;  $t$  is the time in s (second).

The solution to (4) must satisfy next boundary conditions:

The boundary condition of the 1st kind (temperature values are specified) at the boundary  $S_T$ :

$$T = f(x, y, z) \quad (5)$$

The boundary condition of second kind (heat flow is given) at the boundary  $S_q$ :

$$-\left( \lambda_x \frac{\partial T}{\partial x} l_x + \lambda_y \frac{\partial T}{\partial y} l_y + \lambda_z \frac{\partial T}{\partial z} l_z \right) = q \quad (6)$$

where  $l_x$ ,  $l_y$ ,  $l_z$  are direction cosines according to  $x$ ,  $y$ ,  $z$  axis;  $q$  is heat flux density in  $\text{Wt}/\text{m}^2$ .

The boundary condition of third kind (convective heat exchange is given) at the boundary  $S_h$ :

$$-\left( \lambda_x \frac{\partial T}{\partial x} l_x + \lambda_y \frac{\partial T}{\partial y} l_y + \lambda_z \frac{\partial T}{\partial z} l_z \right) = h(T - T_0) \quad (7)$$

where  $T_0$  is the cooling air temperature in K.

### D. Determination of the Rotor Blades Forced Vibration Frequency

The dependence between the blades surface temperature and their surface displacement is given in paper [24]. Thus, the vector of each finite element, forming the rotor, generalized displacement consists of the mechanical  $\delta_m$  and thermal displacements  $\delta_T$ :

$$\boldsymbol{\delta} = \begin{bmatrix} \delta_m \\ \delta_T \end{bmatrix} \quad (8)$$

Thus putting (8) and (3) into (1), we can find the dependence between the rotor temperature and centrifugal force and its forced vibration frequency:

$$\det|\mathbf{K} + \mathbf{C}| - f^2 \mathbf{M} = \mathbf{p} + \mathbf{F} \quad (9)$$

where  $f$  is the rotor blades forced vibration frequency.

## V. MATHEMATICAL MODEL EXPERIMENTAL VERIFICATION

### A. Description of the Highly Automated Holographic Experimental Equipment

The experimental study of the frequency and modal spectra was carried out using the contactless coherent-optical method of holographic interferometry [4, 11]. The optical scheme and block diagram of the experimental setup are shown on Fig. 2.

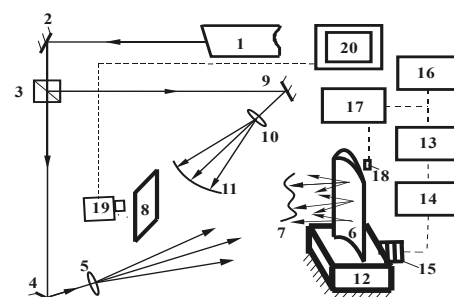


Fig. 2. Highly automated holographic experimental equipment.

The beam of He-Ne laser 1 with a power of 50 mW and a wavelength of  $\lambda = 0.63 \mu\text{m}$  is reflected by a flat mirror 2 and is divided into two beams by a beam splitter cube 3. The beam that has passed through the beam splitter is reflected by a flat mirror 4, expanded by an objective 5, and illuminates a blade 6. The light wave 7 scattered by the diffuse surface creates an object light beam on a photographic plate 8. The beam reflected by the beam splitter is directed by mirror 9 to microlens 10 and forms a spherical reference wave 11. The result of the interference of the converging reference and object waves is recorded

by high-resolution photographic plate 8 and forms a hologram.

The blade 6 was fixed in a special clamp 12, providing rigid fixation of its root section. A sinusoidal vibration excitation signal is generated by a sound generator 13 and, after amplification by a low-frequency amplifier 14, is fed to a piezoceramic wave-type exciter 15, mounted in the clamping device. The exciter pusher rests against the clamping element of the lock, exciting in it deformation waves, that are transmitted to the blade. It is important that this eliminates the influence of the exciter on the forced vibration frequencies and vibration modes and minimizes the possibility of skipping resonant modes. The vibration excitation frequency is determined automatically by an electronic frequency meter 16, and the occurrence of vibrations with multiple frequencies is monitored by an oscilloscope 17. For this purpose, a signal from a contactless vibration sensor 18, recording vibrations of the peripheral point of the blade feather, is fed to the first input of the oscilloscope, and an excitation signal is fed to the second input. The forced vibration frequencies were determined by automatic observing holographic vibration interferograms in real time. For this purpose, a highly digitalized video camera 19 displays the interferogram image on computer screen 20. Since the vibration frequency significantly exceeds the frame rate of the camera, this image is automatically averaged by the video system during frame recording. In this way, the resonance mode of vibration is adjusted and the frequency spectrum is determined.

#### B. Mathematical Model Verification

To verify the developed mathematical model an experimental investigation for the turbine rotor first impeller blades forced vibration modes and frequencies have been determined. During the experiment the blade surface temperature was equal to the ambient temperature. Some forced vibration modes for the turbine blades of first impeller received by the method of real time speckle interferometry are given below.

The given vibration modes can show us the strain distribution on the blades surface caused by the forced vibration process. The bright white stripes show the places with zero deformation, so they can be considered as a neutral axis of the blade. But on the other hand, these parts of the blade surface are the stress concentrators. Data shown on the Fig. 3 gives us an opportunity to realize that the location of stress concentrators changes for each mode. Thus, it can be concluded that the stress concentration blades durability and vibration mode strictly depended from the vibration frequency. Special attention should be paid to the various parameters' influence on the forced vibration frequencies value.

Experimental results of the blades forced vibration frequencies determination in comparison with the calculated data are given in the Table I.

Studying the results, presented in Table I we find out that the discrepancy between the numerical and experimentally found data is lower than 10%. It gives us an opportunity to make a conclusion, that the developed mathematical model is verified and adequate. So, it can be used for studying the forced vibration of the marine gas turbine rotor blades.

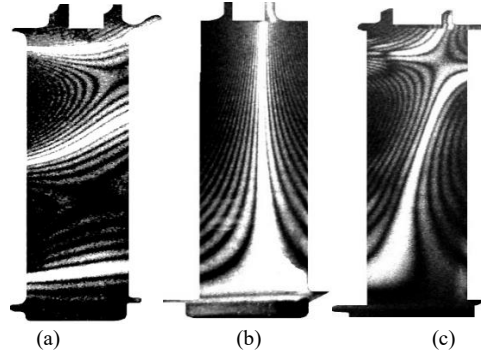


Fig. 3. Experimentally determined forced vibration modes for the first impeller turbine blade: (a)  $m=0, n=3$  vibration mode, (b)  $m=1, n=1$  vibration mode, (c)  $m=1, n=2$  vibration mode.

TABLE I: COMPARISON OF THE FIRST IMPELLER BLADES FORCED VIBRATION FREQUENCY EXPERIMENTAL AND CALCULATION DATA

Forced vibration modes	Forced vibration frequency $f$ , Hz Numerical / Experimental data	Divergence, %
$m=0, n=3$	812.5 / 807.12	6.3
$m=1, n=1$	1968.9 / 1791.65	7.8
$m=1, n=2$	2044.6 / 2022.81	9.6

## VI. RESULTS AND DISCUSSION

The power of the investigated gas turbine is 25 MW. The gas temperature at the entrance to the turbine rotor is 1583 K; total pressure at the stage inlet 0.7578 MPa; rotor angular velocity is near 11000 r/min; the blades material density  $\rho = 8100 \text{ kg/m}^3$ ; Young modulus  $E = 1.693 \times 10^{11} \text{ Pa}$ ; Poisson ratio  $\nu = 0.3$ . The maximum gas turbine rotor shaft angular velocity  $\Omega = 11000 \text{ rpm}$ .

The set of calculations has been held. Firstly, we determine the influence of temperature, centrifugal force and blades constructional damping parameters on the rotor forced vibration frequency. Then the blades durability under the complex influence of forced vibration, thermal state and centrifugal force has been studied.

#### A. Influence of the Gas Flow Temperature and Centrifugal Force

Results of the studies are given in the following tables. The cooled blades of the first, most highly loaded impeller have been taken into consideration.

TABLE II: INFLUENCE OF THE GAS FLOW TEMPERATURE ON THE FIRST IMPELLER BLADES FORCED VIBRATION FREQUENCY

Forced vibration modes	Forced vibration frequency $f$ , Hz	Blades surface temperature $T, ^\circ\text{C}$
$m=0, n=1$	1012.5	
$m=1, n=1$	2468.9	500
$m=1, n=2$	2644.6	
$m=0, n=1$	1001.1	
$m=1, n=1$	2268.8	750
$m=1, n=2$	2391.9	
$m=0, n=1$	812.4	
$m=0, n=1$	183.2	1000
$m=0, n=1$	2688.9	

The data presented in the Table II shows that the turbine blades forced vibration is influenced by the high temperature. The increase of the temperature leads to the smooth gradual decrease of the blades forced vibration. This can be explained by the influence of the damping,

caused by the beginning of creep processes in the blades feather material.

Then the influence of the centrifugal force on the first impeller blades forced vibration parameters is studied. The highest possible angular velocity on the turbine normal regime is taken into account.

TABLE III: INFLUENCE OF THE CENTRIFUGAL FORCE ON THE FIRST IMPELLER BLADES FORCED VIBRATION FREQUENCY

Forced vibration modes	Forced vibration frequency $f$ , Hz	Blades surface temperature $T$ , °C	Angular velocity $\Omega$ , r/min
$m=0, n=1$	1139.60		
$m=1, n=1$	2574.20	500	
$m=1, n=2$	2718.50		
$m=0, n=1$	1065.90		
$m=1, n=1$	2312.80	750	11000
$m=1, n=2$	2456.90		
$m=0, n=1$	868.20		
$m=0, n=1$	1876.70	1000	
$m=0, n=1$	2090.80		

As it is obvious from the data, presented in Table III, taking into account the centrifugal force at the rotor normal regime increases the blades forced vibration. Such increase is not sharp and is not more than 10% in comparison with the frequencies calculated without taking into account the centrifugal force.

#### B. Influence of the Blades Constructional Damping Parameters

The mounting tension on the blades bandages during technological operations of assembling the impeller is set using the bandage twist angle  $\theta$ . Twisting occurs in accordance with the positive direction of the x axis of the global rotor coordinate system. Therefore, before considering the influence of the design parameters of the blades bandages on the impeller forced vibration frequency at the first, we will analyze the dependence of the forced vibration frequency on the magnitude of this angle. The studies were conducted for the vibration mode  $m=1, n=2$ , which was previously determined as the most dangerous from the point of view of the impeller vibration according to the Table III. The studies were held for the rotor first impeller (Fig. 1).

TABLE IV: INFLUENCE OF THE MOUNTING TENSION ANGLE ON THE FIRST IMPELLER BLADES FORCED VIBRATION FREQUENCY

Mounting tension twist angle $\theta$ , degree	Forced vibration frequency $f$ , Hz
0	3125.0
1.0	3133.5
1.5	3143.8
2.0	3145.9
2.5	3156.2
3.0	3168.9
4.0	3172.1
4.5	3183.7

Analysis of the data shown in Table IV allows us to conclude that the installation tension is more significant for the first impeller. This is explained by the fact that

increasing the stiffness of the blade impeller by means of installation tension leads to an approximation of the boundary conditions for fixing the blade to the C - C type. Therefore, the frequency of forced vibration of the impellers also increases. According to the design, the first blade impeller is the most rigid, and therefore for its frequency of forced vibration increases. Therefore, based on the analysis of Table IV we can conclude that the optimal option is to assemble the impeller with the bandages twist angle  $\theta$ , which is in the range from 1.5 degrees to 4.5 degrees. This will ensure sufficient stiffness of the blade connection with the simultaneous possibility of using constructive damping to reduce the frequency of the impeller forced vibration. Therefore, in further calculations, we will assume that the angle  $\theta$  will be 4.5 degrees.

Next, we will consider the influence of the geometric characteristics of the bandages, which can affect the level of constructive damping. Based on the design of the bandage, the thickness and width of the bandage are the most important parameters.

Analysis of the data given in Table V and Table VI allows us to understand the influence of constructive damping on the first impeller forced vibration frequencies. It is clear that the influence of the width of the contact zone is more significant, because the slippage length depends on the value of such a parameter. So, from Table V it can be seen that for the all modes of the impeller forced vibration the difference between the forced vibrations frequencies for the largest and smallest widths, due to the design of the side surfaces of the bandage, is 61 Hz. But, on the other hand, a significant increase in the width of the contact zone in turn leads to an increase in the assembly tension during the technological operations of impeller assembling. As a result, increases its rigidity and the vibration frequency.

TABLE V: INFLUENCE OF THE CONTACT ZONE WIDTH ON THE FIRST IMPELLER BLADES FORCED VIBRATION FREQUENCY

Forced vibration modes	Width of the contact zone, mm		
	5.0	7.5	10.0
Forced vibration frequency $f$ , Hz			
$m=0, n=1$	887.14	876.18	868.27
$m=1, n=1$	1900.03	1891.14	1876.70
$m=1, n=2$	3041.81	3005.98	2090.82

TABLE VI: INFLUENCE OF THE BLADES BANDAGES CONTACT ZONE THICKNESS ON THE FIRST IMPELLER BLADES FORCED VIBRATION FREQUENCY

Forced vibration modes	Thickness of the bandage contact zone, mm		
	2.5	2.65	2.8
Forced vibration frequency $f$ , Hz			
$m=0, n=1$	884.16	875.39	821.43
$m=1, n=1$	1892.80	1889.47	1873.71
$m=1, n=2$	3008.48	3001.58	2087.85

The data from Table V also make it possible to understand the influence of the thickness of the bandage on the impeller forced vibration frequencies. We also see that an increase in the bandage thickness leads to a decrease of the forced vibration frequencies, although this influence is not as significant as the width of the contact zone. For the most dangerous mode, the difference

between the vibration frequencies according to the largest and smallest thicknesses is only 18 Hz. With an increase in the thickness of the bandage, vibration frequency decreases, but a significant increase in the thickness of the bandage also leads to a significant increase in its stiffness and, as a result, the impeller forced vibration frequency begins to increase too.

The novelty of the work in comparison with the most recent papers [1–3] is in the usage of three-dimensional curvilinear finite elements for the blade approximation, special experimental laser equipment and study of the blade bandages damping influence on their forced vibration frequencies and durability. It was also found out that the mounting tension angle for all types of the impellers must not exceed the value of 5 degrees, because the higher values of this angle decrease the area of the bandages surface friction.

### C. Determination of the Blades Durability

Next step is the determination of the rotor first impeller blades durability under the complex influence of such negative factors as forced vibration, high temperature and centrifugal force.

Data, presented in Table VII, gives an opportunity to make a decision that the blades durability sharply (several hundred times) decreases under the complex negative influence of forced vibration, high temperature and centrifugal force. Furthermore, it should be taken into account that the obtained numerical data don't have a big divergence with the results of experimental investigation of turbine blades durability, given in paper [25], that verifies the developed mathematical model and proves its adequacy.

TABLE VII: DETERMINATION OF THE FIRST IMPELLER BLADES DURABILITY UNDER THE COMPLEX INFLUENCE OF FORCED VIBRATION, HIGH TEMPERATURE AND CENTRIFUGAL FORCE

Forced vibration modes	Forced vibration frequency $f$ , Hz	Blades surface temperature $T$ , °C / Angular velocity $\Omega$ , rev/min	Durability (number of cycles till blades crack process begining) $N$
$m=0, n=1$	1139.60		
$m=1, n=1$	2574.20	500 / 5000	$1.54 \times 10^8$
$m=1, n=2$	2718.50		
$m=0, n=1$	1065.90		
$m=1, n=1$	2312.80	750 / 8500	$2.97 \times 10^7$
$m=1, n=2$	2456.90		
$m=0, n=1$	868.20		
$m=0, n=1$	1876.70	1000 / 11000	$5.14 \times 10^6$
$m=0, n=1$	2090.80		

## VII. CONCLUSION

The durability of turbine rotors used for various power plants has been studied. For this purpose, a more precise mathematical model taking into account exciting gas dynamic force and impeller forced vibration amplitudes was developed. On its base, the problems of the constructional damping influence on the impellers forced vibration amplitudes and frequencies have also been studied. The developed mathematical model has been experimentally verified.

The rotor blades forced vibration, caused by gas flow temperature and centrifugal force on the blades forced

vibration frequencies have been studied for the three first vibration modes. It has also been found that the main factors, causing the reduction of the impellers forced vibration frequency, are the types of connection between the blades bandages. In the existing mathematical models [1, 2, 15, 19–21], such information is not present. Using the developed mathematical model, it was found out that the sharp decrease of the impellers forced vibration frequency is caused by the slippage at the bandages contacting surfaces. Also, for the marine gas turbine engines designers is extremely important that the most useful from the rotor vibrodurability point of view blades bandages parameters are: bandage contact zone thickness 2.8 mm, contact zone width 10 mm. Amplitudes of the impeller forced vibration have been found taking into account the processes of friction on the blade bandages contacting surfaces.

Results of the study with the high level of dynamic stresses strongly demand to continue researches taking into account the turbine rotor creep and fatigue destruction problems. Also, it should be mentioned that the developed mathematical model has some limitations. It doesn't take into account the friction in material and the heat flux increase due to such friction. Thus, it can't be used for blades made from viscoplastic materials.

## CONFLICT OF INTEREST

The authors declare no conflict of interest.

## AUTHOR CONTRIBUTIONS

Serhii Morhun and Natalia Smetankina conducted the research; Iryna Zhuk and Yurii Zolotoi developed the experimental equipment. Serhii Morhun and Mahmoud M. S. Al-suod analyzed the data; Nour Hider Almarahle and Razan Haedar Al marahla wrote the paper. All authors had approved the final version.

## REFERENCES

- [1] G. Nan, X. Yao, S. Yang *et al.*, "Vibrational responses and fatigue life of dynamic blades for compressor in gas turbines," *Engineering Failure Analysis*, vol. 156, 107827, Feb. 2024.
- [2] C. X. Chen, Z. Wang, N. Yang *et al.*, "Shock response prediction and anti-shock optimization for full coupled gas turbine," *International Journal of mechanical Sciences*, vol. 303, 110640, Oct. 2025.
- [3] C. C. Tran, "Fatigue life and modal analysis of centrifugal fan's impeller in portable pneumatic extinguisher for forest fires," *Journal of Research and Applications in Mechanical Engineering*, vol. 13, no. 1, pp. 1–10. 2025.
- [4] G. Cubrel, P. Psota, P. Dancova *et al.*, "Digital holographic interferometry for the measurement of symmetrical temperature fields in liquids," *Photonics*, vol. 8, no. 6, pp. 200–212. 2021.
- [5] P. Psota, H. Tang, K. Pooladvand *et al.*, "Multiple angle digital holography for the shape measurement of the unpainted tympanic membrane," *Optics Express*, vol. 28, no. 17, pp. 24614–24628, 2020.
- [6] A. I. Balitskii, V. V. Dmytryk, L. M. Ivaskevich *et al.*, "Improvement of the mechanical characteristics, hydrogen crack resistance and durability of turbine rotor steels welded joints," *Energies*, vol. 15, no. 16, pp. 6006–6014, 2022.
- [7] J. D. Quadros, P. Thalambeti, M. M. Ndiaye, and I. Yakub, "Performance analysis of a gas turbine engine with intercooling and regeneration process - Part 1," *International Journal of Turbo and Jet Engines*, vol. 42, no. 1, pp. 23–31, 2025.

- [8] O. Alsmadi, Z. Abu-Hammour, and K. Mahafzah, "Digital systems model order reduction with substructure preservation and fuzzy logic control," *The Eurasia Proceedings of Science, Technology, Engineering & Mathematics*, vol. 28, pp. 14–22, 2024. doi: 10.55549/epstem.1519121
- [9] K. A. Mahafzah, M. A. Obeidat, A. M. Mansour *et al.*, "Artificial-intelligence-based open-circuit fault diagnosis in VSI-Fed PMSMs and a novel fault recovery method," *Sustainability*, vol. 14, no. 24, 2022. <https://doi.org/10.3390/su142416504>
- [10] M. I. Alamayreh, A. Fenocchi, G. Petaccia, S. Sibilla, and E. Persi, "Numerical analysis of fluid flow dynamics around a yawed half-submerged cylinder inside an open channel," *Journal of Hydrodynamics*, vol. 33, no. 1, pp. 111–119, 2021.
- [11] Y. Wang, M. Zhu, S. Zhang Qiang, X. Zheng, and J. Teng, "Numerical and experimental study on the critical geometric variation based on sensitivity analysis on a compressor rotor," *International Journal of Turbo and Jet Engines*, vol. 42, no. 1, pp. 115–128, 2025. <https://doi.org/10.1515/tjj-2023-0097>
- [12] M. A. Kenanda, F. Hammadi, and W. Zouari, "Thermo-mechanical free vibration analysis of porous solar FGM plates resting on Kerr's foundation using a new logarithmic-hyperbolic shear deformation theory," *Archive of Applied Mechanics*, vol. 95, pp. 91–99, 2025. <https://doi.org/10.1007/s00419-025-02779-7>
- [13] S. Seok, A. Shahriar, and A. Montoya, "A finite element approach for simplified 2D nonlinear dynamic contact impact analysis," *Archive of Applied Mechanics*, vol. 93, pp. 3511–3531, 2023. <https://doi.org/10.1007/s00419-023-02451-y>
- [14] B. Arnab, S. Prabhakar, and C. Giacomo, "Natural frequency analysis of a functionally graded rotor-bearing system with a slant crack, subjected to thermal gradients," *International Journal of Turbo and Jet Engines*, vol. 40, no. 3, pp. 243–255, 2023.
- [15] L. Shakurova, I. Armenise, and E. Kustova, "Effect of slip boundary conditions on nonequilibrium reacting air flows," *Journal of Theoretical and Applied Mechanics*, vol. 53, no. 3, pp. 253–269, 2023.
- [16] S. Wang, L. Shouzuo, L. Lei, Z. Zhao, D. Wei, and S. Bengt, "A high temperature turbine blade heat transfer multilevel design platform," *Numerical Heat Transfer, Part A: Applications*, vol. 79, no. 2, pp. 122–145, 2021.
- [17] K. G. Aktas, F. Pehlivan, and I. Esen, "Temperature-dependent thermal buckling and free vibration behavior of smart sandwich nanoplates with auxetic core and magneto-electro-elastic face layers," *Mechanics Time-Dependent Materials*, vol. 28, pp. 1999–2039, 2024. <https://doi.org/10.1007/s11043-024-09698-0>
- [18] Z. A. Duriagina, V. V. Kulyk, O. S. Filimonov, A. M. Trostianchyn, and N. B. Sokulska, "The role of stress-strain state of gas turbine engine metal parts in predicting their safe life," *Progress in Physics of Metals*, vol. 22, no. 4, pp. 643–677, 2021.
- [19] A. N. Guz, V. L. Bogdanov, and V. M. Nazarenko, "Three-dimensional problems on loading of bodies along cracks," *Advances in Structure Materials*, vol. 138, pp. 239–249, 2020. [https://doi.org/10.1007/978-3-030-51814-1\\_4](https://doi.org/10.1007/978-3-030-51814-1_4)
- [20] N. Navadeh, I. Goroshko, Y. Zhuk, E. M. Farnoosh, and S. F. Arash, "Finite element analysis of wind turbine blade vibrations," *Vibration*, vol. 4, no. 2, pp. 310–322, 2021.
- [21] L. Lu and L. Zhang, "Study on vibration characteristics of wind turbine rotor blades based on ANSYS," in *Proc. the 2018 7th International Conference on Energy and Environmental Protection*, 2020. doi: 10.2991/iceep-18.2018.149
- [22] F. A. X. C. Pinho, M. Amabili, and Z. J. G. N. Del Prado, "Nonlinear forced vibration analysis of doubly curved shells via the parameterization method for invariant manifold," *Nonlinear Dynamics*, vol. 112, pp. 20677–20701, 2024. <https://doi.org/10.1007/s11071-024-10135-7>
- [23] S. Morhun and S. Vilkul, "Gas dynamic analysis of the modern single shaft gas turbine engine flow path," *International Journal of Turbo and Jet Engines*, vol. 40, no. s1, pp. 271–278, 2023.
- [24] S. Morhun, "Determination of the modern single shaft gas turbine rotor thermal stresses," *Journal of Theoretical and Applied Mechanics*, vol. 54, pp. 46–50, 2024. <https://doi.org/10.55787/jtams.24.54.1.046>
- [25] N. Smetankina and S. Morhun, "Determination of the modern marine single shaft gas turbine rotor blades fatigue strength parameters," *International Journal of Turbo and Jet Engines*, vol. 42, no. 2, 271–276, 2025.

distributed under the Creative Commons Attribution License (CC BY 4.0), which permits use, distribution and reproduction in any medium, provided that the article is properly cited, the use is non-commercial and no modifications or adaptations are made.



**Nour Hider Almarahleh** is with Civil Engineering Department, Tafila Technical University. Currently she is an assistant professor of structure engineering. She got the PhD in structural engineering, Western Michigan University, USA. Her research interest is reinforced concrete structures; concrete members reinforced with FRP bars, earthquake, concrete deformations under sustained stresses, structural dynamics, finite element, and machine learning.



**Mahmoud M. S. Al-suod** is an associate professor in Power and Mechatronics Department at Tafila Technical University from 2020–now. He is an assistant professor in Power and Mechatronics Department at Tafila Technical University from 2014–2020. He received his PhD, MSc and B.Sc. in electrical engineering, Admiral Makarov National University of Shipbuilding in 2013, 2009 and 2007 respectively. His research of interest the automation of electric power systems, information provision of electric power systems, control.



**Serhii Morhun** is an associate professor in Engineering Mechanics and Technology of Machinebuilding Department at Admiral Makarov National University of Shipbuilding from 2019–now. He received his Ph.D., M.Sc. and B.Sc. degrees in applied mechanics, Admiral Makarov National University of Shipbuilding in 2015, 2010, and 2008, respectively. His interests are the gas turbine engines rotors flow dynamics, heat exchange, forced vibration, dynamic and fatigue strength and creep.



**Natalia Smetankina** is the head of Department of Vibration and Thermostability Studies at the Anatolii Pidhornyi Institute of Power Machines and Systems of the National Academy of Sciences of Ukraine in Kharkiv. She received her full prof., DSc and PhD (solid mechanics) at the Anatolii Pidhornyi Institute of Power Machines and Systems of the National Academy of Sciences of Ukraine in 2023, 2012, 1998, and MSc (dynamics and strength of machines) in National Technical University «Kharkiv Polytechnic Institute» in 1991. Her research focuses on the integration of theoretical and applied approaches for simulating the mechanical behavior, durability, and failure mechanisms of structural systems under coupled multiphasic loading conditions.



**Irina Zhuk** is a senior lecturer at the Department of Hygiene, Social Medicine, Public Health, and Medical Informatics at Petro Mohyla Black Sea National University. Her scientific interests include on automated systems and computer literacy, laser measurement techniques, holographic and speckle interferometry, as well as vibration research.



**Yuriii Zolotyi** is the head of the laboratory in Engineering Mechanics and Technology of Machinebuilding Department at Admiral Makarov National University of Shipbuilding. His scientific interests focus on laser measurement techniques, holographic and speckle interferometry, as well as vibration research



**Razan Haedar Al Marahla** is with Civil and Infrastructure Engineering Department, Al-Zaytoonah University of Jordan. Currently she is an assistant professor of concrete engineering & structure. She got the PhD in structural engineering, University of Leeds, UK. Her research interests are reinforced concrete structures, concrete members reinforced with FRP bars, short and time-dependent flexural behavior of FRC-FRP (deflection and cracking performance), concrete deformations under sustained stresses, and structural dynamics.